JOURNAL OF GUIDANCE, CONTROL, AND DYNAMICS
Vol. 30, No. 1, January–February 2007

Adaptive Deflection-Limiting Control for Slewing Flexible Space Structures

Hirohisa Kojima
Tokyo Metropolitan University, Tokyo 192-0397, Japan
and
William Singhose
Georgia Institute of Technology, Atlanta, Georgia 30332

DOI: 10.2514/1.23668

This paper proposes an adaptive deflection-limiting input shaping technique for slewing flexible space structures. The bending moment at the root of the flexible appendage is measured and used to adjust the control parameters. This measurement is more easily obtained than the tip acceleration on a space structure and it is very useful for avoiding damage to the flexible structure. The control timing of the input shaping is automatically tuned during the slewing motion to limit the induced bending moment and to eliminate the residual vibration. The effectiveness of the adaptive deflection-limiting input shaping control is verified experimentally and compared with the traditional input shaping control methods.

I. Introduction

SPACE structures are required to be as light as possible to reduce launch cost, but their size must be maximized to contain as many mission devices as possible. It is impossible to ignore the flexibility of space structures during maneuvers because of the interaction between the attitude motion and flexible motion. Therefore, many control methods have been proposed to suppress vibrations of flexible space structures during maneuvering.

Input shaping is one such control method, which uses a sequence of impulses as the representative form of the control input. However, real systems cannot be actuated by a sequence of impulse commands; they require finite duration command signals. Thus, the properties of the impulse command need to be converted to a finite duration command. This conversion can be accomplished by convolving the sequence of impulses with any command. This convolution process is demonstrated in Fig. 1.

There are various versions of the input shaping control technique, such as zero vibration (ZV) [1,2], zero vibration and derivative (ZVD) [2], specified insensitivity (SI) [3], and the extra-insensitive (EI) approach [4]. These input shaping techniques can suppress residual vibrations as long as the system parameters are well known, or the change in modeling parameters is limited to within a reasonable bound. However, if the system has a large range of unknown or varying frequencies, then another approach is needed to make the control methods more robust. Tzes and Yurkovich [5] and Khorrami et al. [6] have proposed online adaptive schemes to update the input shaper parameters. Bodson [7] has used a recursive least-squares technique to tune the input shaper parameters. Magee and Book [8] have proposed a method in which the input shaper is modified as a function of the system configuration.

Although these adaptive input shapers can eliminate or suppress residual vibrations in case of parameter uncertainties, they do not consider the transient load [9,10] on the flexible structure during maneuvers. If the transient deflection is greater than acceptable limits, then it may damage the structure. To overcome this problem, deflection-limiting (DL) input shaping [11,12] has been proposed. Original DL shapers, however, do not have the ability to automatically tune their performance to the system parameters during maneuvers. Therefore, adaptive methods need to be added to DL shapers for systems with large uncertainties. This paper proposes an adaptive deflection-limiting input shaping control for slewing flexible space structures. In addition, the necessary relationship between the oscillation frequencies and the deflection limit required for feasible implementation of the adaptive deflection-limiting control is derived.

In the adaptive deflection-limiting (ADL) control proposed in this paper, the first modal frequency is estimated from the second modal frequency which is determined by the empirical transfer function estimate (ETFE) technique [13]. Then, the timing and amplitude of the impulses of the input shaper are immediately tuned in accordance with the identified frequencies and the measured magnitude of vibration. Furthermore, to achieve the desired final maneuver angle, the command switch times are tuned in accordance with the measured slewing angle.

Contrary to previous work that used measurements of a flexible beam's tip acceleration to adjust the input shaper parameters, here the bending moment at the root of the beam is measured and used to adjust the parameters. This measurement may be more easily obtained than the tip acceleration on a space structure. In addition, measuring and limiting the bending moment at the root is useful for avoiding damage to the flexible structure. The experimental results presented later in this paper show that the adaptive deflection-limiting control method can successfully suppress the bending moment at the root of the beam during maneuver and greatly reduce the residual vibrations.

II. Adaptive Deflection-Limiting Input Shaping

A. Input Shapers

Before explaining deflection-limiting shapers, general input shaping concepts are reviewed. To simplify the analysis, only one flexible mode is considered here. If a system's natural frequency ω

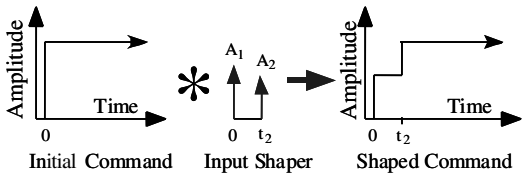

Fig. 1 Input shaping.

Received 6 March 2006; revision received 2 June 2006; accepted for publication 2 June 2006.

*Also Tokyo Metropolitan Institute of Technology, Associate Professor; hkojima@cc.tmit.ac.jp (corresponding author).
†Associate Professor; Singhose@gatech.edu.

and damping ratio ζ are estimated reasonably, then the nondimensional residual vibration that results from a sequence of impulses being applied to the system can be described by [2]

$$V(\omega,\zeta) = e^{-\zeta\omega t_n}\sqrt{C(\omega,\zeta)^2 + S(\omega,\zeta)^2} \tag{1}$$

where

$$C(\omega,\zeta) = \sum_{i=1}^{n} A_i e^{\zeta\omega t_i}\cos(\omega_d t_i) \tag{2a}$$

$$S(\omega,\zeta) = \sum_{i=1}^{n} A_i e^{\zeta\omega t_i}\sin(\omega_d t_i) \tag{2b}$$

A_i and t_i are the amplitude and time location of the ith impulse, n is the number of impulses in the impulse sequence, and $\omega_d = \omega\sqrt{1-\zeta^2}$. By setting (1) to zero and solving it for the impulse amplitudes and time locations, we can determine the desired impulse sequence. For (1) to be zero, both (2a) and (2b) must equal zero independently. Therefore, the impulses must satisfy

$$\sum_{i=1}^{n} A_i e^{\zeta\omega t_i}\cos(\omega_d t_i) = 0 \tag{3a}$$

$$\sum_{i=1}^{n} A_i e^{\zeta\omega t_i}\sin(\omega_d t_i) = 0 \tag{3b}$$

These constraints contain $2n$ unknown parameters. Without loss of generality, the first impulse time, t_1, can be set to be zero. The number of unknown parameters is thereby reduced to $2n-1$.

If the impulse sequence causes no residual vibration, then the convolved command, such as that shown in Fig. 1, will induce no vibration. This convolution also ensures that the rigid-body motion induced by the input remains the same before and after convolution, provided that the input shaper satisfies

$$\sum_{i=1}^{n} A_i = 1 \tag{4}$$

There are now three constraint equations in Eqs. (3a), (3b), and (4). Thus, if the number of impulses is two, then all the unknown parameters can be determined. For input shapers containing additional impulses, additional constraints are needed and can be used to increase robustness of input shaping to modeling errors [2].

B. Deflection-Limiting Control

Deflection-limiting command shapers are a modification of traditional input shapers. Input shapers are usually required to sum to unity to ensure that the unshaped and shaped commands have the same final setpoint. However, if this setpoint leads to excessive transient deflection, then the impulse magnitude requirement must be adjusted. In the deflection-limiting control method described here, the deflection of the first modal frequency is limited, but the second mode of the flexible appendage is not limited. This is because the first mode dominates the transient deflection amplitude. Figure 2 shows one form of the deflection-limiting shaper applied to an acceleration command. The final value of the shaped acceleration is lower than the original value. Therefore, when the shaped command is used in place of the original command, the final deflection is smaller.

Given that a rest-to-rest maneuver is antisymmetric with respect to the midpoint of the maneuver time, the deflection-limiting input shaper proposed here has eight command switch times, as shown in Fig. 3, and represented as an input shaper by

$$\begin{bmatrix} A_i \\ t_i \end{bmatrix} = \begin{bmatrix} 1 & -1 & A_3 & -A_3 & -A_3 & A_3 & -1 & 1 \\ t_1 & t_2 & t_3 & t_4 & t_5 & t_6 & t_7 & t_8 \end{bmatrix} \tag{5}$$

The challenge is to find the eight command switch times and the amplitude, A_3, such that the transient deflection is limited, the residual vibration is eliminated, and the system moves the desired amount. The strategy proposed here is to design the first half of the command to control deflection and vibration. Then, use an antisymmetrical command to decelerate the system, and arrive at the desired location. Therefore, the first step is to accelerate the system without exceeding the deflection limit and without inducing residual oscillation. This can be accomplished by ensuring the first three impulses combine to produce zero vibration.

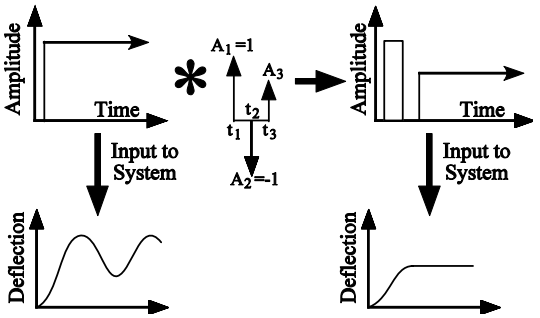

Fig. 2 Deflection-limiting shaper.

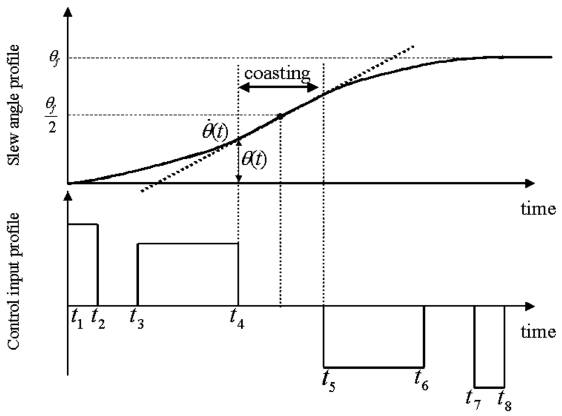

Fig. 3 Sequence of deflection-limiting control for rest-to-rest maneuver.

Setting Eqs. (3a) and (3b) equal to zero at the third command switch time, t_3, yields

$$1 - \cos(\omega_d t_2) + A_3\cos(\omega_d t_3) = 0 \tag{6a}$$

$$-\sin(\omega_d t_2) + A_3\sin(\omega_d t_3) = 0 \tag{6b}$$

A_3 is determined, from the deflection limit, as follows [12]:

$$A_3 = 2\mathrm{DL} \tag{7}$$

where DL is the nondimensional deflection limit defined as the ratio between the acceptable deflection and the maximum deflection resulting from the original input. Using Eqs. (6a), (6b), and (7), the second and third command switch times, t_2 and t_3, can be obtained as follows [12]:

$$t_2 = \frac{1}{\omega_d}\cos^{-1}\left(1 - \frac{A_3^2}{2}\right) = \frac{1}{\omega_d}\cos^{-1}(1 - 2\mathrm{DL}^2) \tag{8a}$$

$$t_3 = \frac{1}{\omega_d}\cos^{-1}\left(-\frac{A_3}{2}\right) = \frac{1}{\omega_d}\cos^{-1}(-\mathrm{DL}) \tag{8b}$$

To determine the appropriate value of A_3 to use in an adaptive deflection-limiting control system, a relationship between the applied control input and the deflection of the flexible appendage must be obtained before the second command switch, t_2. In the

following subsection, an adaptive method to obtain this relationship, and tune the parameters in accordance with this relationship will be described.

C. Adaptive Deflection-Limiting Control

Rather than using an extremely robust shaper, which will slow the system response, it is possible to adaptively change a deflection-limiting shaper. An adaptive algorithm must be able to provide the critical information about the first modal frequency before the second command switch time, t_2, in the input shaper. The second command switch time depends on both the first modal frequency and the deflection-limit amplitude, as shown in Eq. (8a). Therefore, the first modal frequency and the relationship between the maximum deflection and the maximum control input must be obtained before the second command switch time.

Measurements of beam deflection taken during less than a half period of the low mode are not sufficient to determine its frequency, when a Fourier analysis is applied. This means that the first modal frequency cannot be directly determined from the output signals within the required time. However, the first modal frequency can be implicitly determined from the ratio between the first modal frequency and the second one, if the beam dynamics are approximately known. In the present study, the second modal frequency is identified using an empirical transfer function estimate [13], which is a nonrecursive updating scheme for the transfer function. Using the real-time calculation of the second mode, the first mode is estimated and used in Eqs. (8a) and (8b) to calculate a shaper that limits deflection and residual oscillation of the first mode.

The adaptive scheme proposed here consists of six steps.

1) The maximum control torque is applied to the system. The input and output signals are recorded until 40% of the allowable deflection appears. When the bending moment reaches 40% of the allowable level, then the time, which is hereafter referred to as t^*, is recorded. Under the assumption that the deflection mainly depends on the first mode, Eqs. (7) and (8a) show that the beam deflection induced by the maximum control input reaches DL times the allowable level at the second command switch t_2. The second command switch t_2 must be determined before this timing. On the other hand, to have enough time to calculate t_2 and use it to shape the control input, the adaptation scheme is initiated at 40% of the allowable deflection.

2) After the time t^* is recorded, the second modal frequency is determined from the recorded data using the fast ETFE.

3) The first modal frequency, ω_1, is calculated from the estimated ratio between the first and second frequencies.

4) The deflection limit is calculated. In general, the maximum deflection starting from the rest state and induced by the continuous maximum control input, $D_{\max}$, can be represented as

$$D_{\max} = 2k \tag{9}$$

where k is the equilibrium deflection with respect to the maximum control torque. On the other hand, because 40% of the allowable deflection, $D^* = 0.4D_{\lim}$, appears at the time t^*, then D^* can be approximately formulated as follows:

$$D^* = 0.4D_{\lim} = k(1 - \cos\omega_1 t^*) \tag{10}$$

where $D_{\lim}$ is the allowable deflection. Because DL is defined as the ratio between the allowable deflection and the maximum deflection induced by the maximum control input, it can be represented as

$$\mathrm{DL}: = \frac{D_{\lim}}{D_{\max}} = \frac{D^*/0.4}{D_{\max}} = 1.25[1 - \cos(\omega_1 t^*)] \tag{11}$$

5) The amplitude of the third impulse, A_3, and the second and the third command switch times, t_2 and t_3, are tuned by Eqs. (7), (8a), and (8b), respectively. The time span between the fourth and fifth command switch times is set to half of the first modal cycle, π/ω_1, so that the vibration induced into the low mode by the change at t_4 is cancelled by the command change at t_5. Because rest-to-rest motion is generally symmetric with respect to the middle point of maneuvering duration, the time spans between the final two command switches are determined as follows:

$$t_7 - t_6 = t_3 - t_2 \tag{12}$$

$$t_8 - t_7 = t_2 \tag{13}$$

6) The remaining time span that is not yet determined is the one between the third and fourth command switch times. This time span can be used to achieve the desired slew angle of the main body, θ_f. For the sake of simplicity, let us temporarily assume that the system is a rigid body and that the slew angle of the main body freely coasts with constant velocity at the time t_4, as shown in Fig. 3. Under these assumptions, the simplest way to tune the fourth command switch time to achieve the desired displacement is to monitor the slew angle $\theta(t)$ and its velocity $\dot{\theta}(t)$ until the condition

$$\frac{\theta_f}{2} - \frac{\pi}{2\omega_1}\dot{\theta}(t) = \theta(t) \tag{14}$$

is satisfied. Then, the time is recorded as t_4, and the time locations of the fifth, sixth, seventh, and eighth command switches are

$$t_5 = t_4 + \frac{\pi}{\omega_1} \tag{15a}$$

$$t_6 = 2t_4 + \frac{\pi}{\omega_1} - t_3 \tag{15b}$$

$$t_7 = 2t_4 + \frac{\pi}{\omega_1} - t_2 \tag{15c}$$

$$t_8 = 2t_4 + \frac{\pi}{\omega_1} \tag{15d}$$

An advantage of this adaptive method is that precise knowledge of the system inertia is not needed to tune the command switch times.

If the deflection does not reach 40% of the allowable level when the slew angle reaches half of the desired slewing angle, then it is not necessary to employ the deflection-limit control. In the present study, this case is not treated. A block diagram of the control strategy is shown in Fig. 4.

D. Required Conditions for Implementation

If the allowable deflection limit is very small, then the implementation of ADL control becomes more difficult because the second command switch time may occur earlier than the time required for determining the second modal frequency. In this subsection, the required conditions for implementation of the ADL control will be derived.

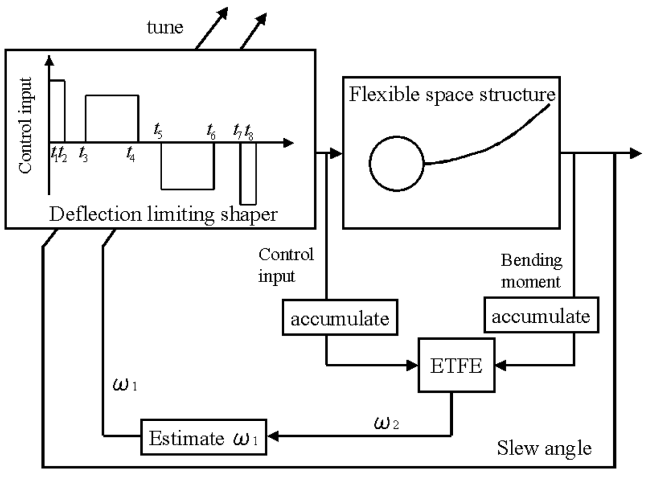

Fig. 4 Block diagram of the adaptive deflection-limiting control.

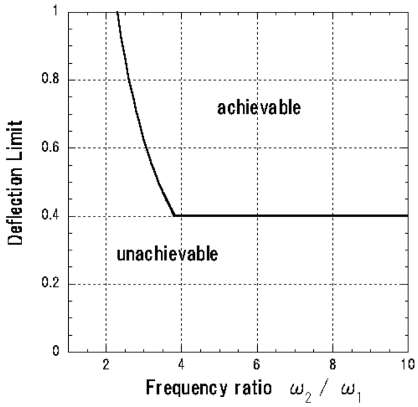

Fig. 5 Required condition between the frequency ratio and deflection limit.

To determine the second modal frequency using ETFE, the half period of the second mode, π/ω_2, must be less than t^*. The time span t^* is obtained from Eq. (11) as

$$t^* = \frac{1}{\omega_1}\cos^{-1}\left(1 - \frac{\mathrm{DL}}{1.25}\right) \tag{16}$$

This must be less than the second command switch. Thus, the required condition becomes

$$\frac{\pi}{\omega_2} < \frac{1}{\omega_1}\cos^{-1}\left(1 - \frac{\mathrm{DL}}{1.25}\right) < \frac{1}{\omega_1}\cos^{-1}(1 - 2\mathrm{DL}^2) \tag{17}$$

This condition can be rewritten as

$$\mathrm{DL} > \max\left\{1.25\left[1 - \cos\left(\frac{\pi}{(\omega_2/\omega_1)}\right)\right], 0.4\right\} \tag{18}$$

Figure 5 indicates the region that satisfies this condition in the space of deflection limit and the frequency ratio, ω_2/ω_1. It should be noted that this condition is ideal, because the time required for the EFTE calculations is ignored. If the necessary calculation time is taken into account, then the practical region becomes smaller than the one indicated in Fig. 5. It can be seen that the unachievable deflection depends on both the frequency ratio and the 0.4 (40%) limit that was selected as the index for implementation of the adaptive deflection-limiting control. In addition, the resolution of the estimated second frequency depends on the sampling time. Thus, the sampling time should be appropriately selected in accordance with the second modal frequency.

III. System Model

Figure 6 shows a model of a space structure consisting of a rigid body and flexible appendage. The appendage is a cantilever beam with one end fixed to the rigid body and the other end free. The rotational and vibrational motion is assumed to be two-dimensional planar motion. The control torque is applied to the center of the rigid body. In the present analysis, the structural damping and the air drag are neglected for the sake of simplicity, and because most space structures are very lightly damped. The kinetic energy of the rotational motion of the system and the potential energy of the flexible appendage due to bending are, respectively, given as

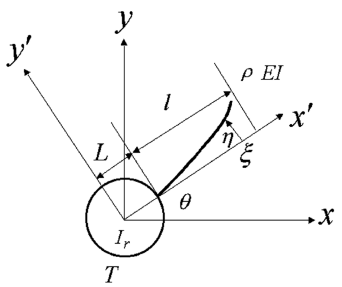

Fig. 6 Model of flexible space structure.

$$K = \frac{1}{2}I_r\dot{\theta}^2 + \frac{1}{2}\rho\int_L^{L+l}(\xi\dot{\theta} + \dot{\eta})^2\,\mathrm{d}\xi \tag{19a}$$

$$U = \frac{\mathrm{EI}}{2}\int_L^{L+l}\left(\frac{\partial^2\eta}{\partial\xi^2}\right)^2\mathrm{d}\xi \tag{19b}$$

where I_r is the moment of inertia, L is the radius of the main body, l is the length of the beam, and EI is the rigidity of the beam. Both l and EI are assumed to be constant along the flexible appendage. The displacement of the beam is denoted by η at the position of ξ. Using Lagrangian theory, the equation of motion for the main body driven by control torque T is obtained as

$$I_r\ddot{\theta} + \rho\int_L^{L+l}\xi(\xi\ddot{\theta} + \ddot{\eta})\,\mathrm{d}\xi = T \tag{20}$$

The behavior of the flexible beam is governed by

$$\mathrm{EI}\,\frac{\partial^4\eta}{\partial\xi} + \rho(\xi\ddot{\theta} + \ddot{\eta}) = 0 \tag{21}$$

with the following boundary conditions:

$$\eta = \frac{\partial\eta}{\partial\xi} \quad \text{at } \xi = L \tag{22a}$$

$$\frac{\partial^2\eta}{\partial\xi^2} = \frac{\partial^3\eta}{\partial\xi^3} = 0 \quad \text{at } \xi = L + l \tag{22b}$$

The flexible vibration of the appendage using assumed vibrational modes can be described as

$$\eta(\xi, t) = \sum\phi_i(\xi)q_i(t) \tag{23}$$

Assuming that vibrational mode variables satisfy

$$\frac{\partial^4\phi_i}{\partial\xi^4} - \beta_i^4\phi_i = 0 \tag{24a}$$

$$\int_L^{L+l}\phi_i\phi_j\,\mathrm{d}\xi = \delta_{ij} \tag{24b}$$

where δ_{ij} is the Kronecker delta, then the equations of motion can be written in the form of the linear time independent (LTI) system as

$$I_r\ddot{\theta} - \mathrm{EI}\sum_{i=1}^{n}\alpha_i\beta_i^4 q_i = T \tag{25a}$$

$$\mathrm{EI}\,\beta_i^4 q_i + \rho(\alpha_i\ddot{\theta} + \ddot{q}_i) = 0 \tag{25b}$$

These equations can be rewritten as

$$\boldsymbol{M}\ddot{\boldsymbol{q}} + \boldsymbol{K}\boldsymbol{q} = \boldsymbol{Q}u \tag{26}$$

where $\boldsymbol{M}$ and $\boldsymbol{K}$ are the mass and rigidity matrix, respectively, $\boldsymbol{q} = [q_i \cdots q_n]^T$ and u is the control input ($u = T$). Considering the eigenvalues of the system, Eq. (26) can be rewritten in the state vector form as follows:

$$\dot{\boldsymbol{x}} = \boldsymbol{A}\boldsymbol{x} + \boldsymbol{B}u \tag{27}$$

where matrices $\boldsymbol{A}$ and $\boldsymbol{B}$ are

$$\boldsymbol{A} = \mathrm{blockdiag}\begin{bmatrix} 0 & 1 \\ -\omega_i^2 & 0 \end{bmatrix} \qquad (i = 0, 1, 2, \ldots, n) \tag{28a}$$

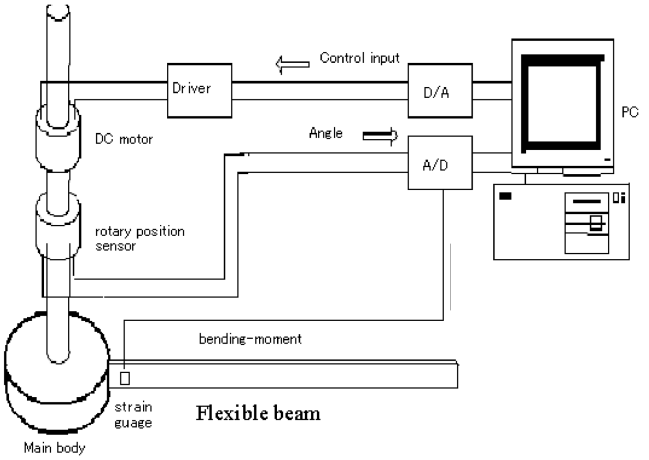

Fig. 7 Experimental setup.

$$\boldsymbol{B} = \begin{bmatrix} 0 & b_0 & 0 & b_1 & \cdots & 0 & b_n \end{bmatrix}^T \tag{28b}$$

and ω_i and b_i are the ith modal frequency and the ith modal gain of the system, respectively. Note that the modal frequencies ω_i are not equivalent to the natural frequencies of the beam alone.

The bending moment at the root of the beam, BM, is represented using the state variables as follows:

$$\text{BM} = \boldsymbol{Cx} \tag{29}$$

where $\boldsymbol{C}$ is the coefficient matrix related to the deflection of the modal vibration.

IV. Experimental Results

A. Experimental Setup

Figure 7 is a diagram of the experimental apparatus. The experiment is set in the horizontal plane to negate the effect of gravity. The flexible appendage is an aluminum beam clamped to a rigid main body that is rotated by a direct current (dc) torque motor. The necessary data for the control, which are the bending moment at the root of the beam and the slew angle of the main body, are provided by two full-bridge strain gauges located at the root of the beam and by a rotary position sensor on the shaft of the motor. The angular velocity of the main body is obtained by numerically differentiating the slew angle with respect to time.

A computer is used to calculate the control input torque in accordance with the control algorithm written in C. The control signal is used to drive the dc torque motor through a digital-analog (D/A) converter, and is converted to electric current by a current amplifier. The sampling frequency for the control signal and measurement is 1000 Hz. The computer processor speed is 2.5 GHz, which is sufficiently fast to estimate the second modal frequency after accumulating enough strain gauge data.

Parameters of the experimental setup are listed in Table 1. Using these parameters, the first and second modal frequencies of the system are analytically estimated as 6.75 rad/s and 39.4 rad/s, respectively. The ratio between these two modal frequencies is 5.84. According to Fig. 5, a deflection limit of 0.5 (50%) is easily achievable for this frequency ratio. The slewing angle is set to 60 deg. Using this slew angle and the system inertia, the calculated slew

Table 1 System parameters

Length of the beam	l	0.845 m
Rigidity	EI	0.175 N · m^2
Mass density	ρ	9.16×10^{-2} kg/m
Moment of inertia	I_r	0.14 kg · m^2
Radius	L	0.0338 m
Maximum torque	——	0.15 N · m
Slew angle	θ_f	60 deg
Deflection limit	DL	1 V (50%)
Sampling rate	——	1000 Hz

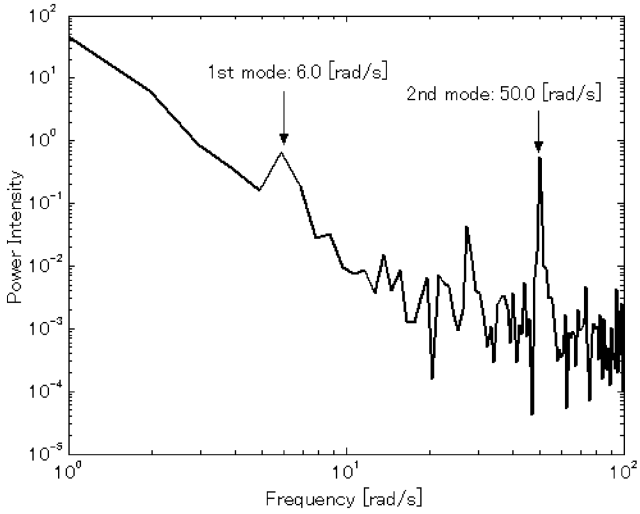

Fig. 8 Result of ETFE using a long data set.

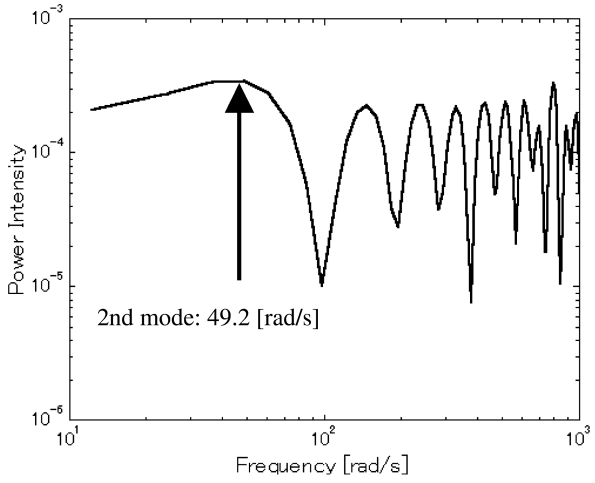

Fig. 9 Result of ETFE using the data only within the time duration t^*.

duration is about 2.0 s. During the maneuver, the first and second modes are estimated to vibrate 1.86 and 10.8 times, respectively. Taking these cycles of vibration and the sampling time into consideration, the number of points used in the ETFE, which should be an Nth power of 2, is selected to be 1024. Although only 80 points of data are sufficient to estimate the second modal frequency, 100 points are used to determine the estimated frequency more precisely, and the rest of the points are zero-padded up to 1024.

B. Experimental Results

The results of the ETFE using a very long data set are shown in Fig. 8, whereas Fig. 9 shows the results when data only within the time t^* are used. The second modal frequency is identified as 49.2 rad/s by the limited data-set ETFE. Using this value, the first modal frequency is estimated as 8.4 rad/s. The experimentally estimated first modal frequency is somewhat greater than the analytical prediction, and slightly less than the one identified by the ETFE using the long data set shown in Fig. 8.

Figure 10 shows the time history of the control input for the case of bang-bang control. The command timing for the bang-bang is calculated based on the system parameters listed in Table 1. The time response of the bending moment at the root of the beam and the time response of the slew angle for the case of bang-bang control are shown in Figs. 11 and 12, respectively.

The absolute maximum bending moment measured by the amplifier in the form of voltage before the half maneuvering time (1.0 s) was about 2.0 V for the bang-bang control. To test traditional deflection-limiting control, the deflection limit is set to 1.0 V; that is, the nondimensional deflection limit is 0.5. The time history of the DL

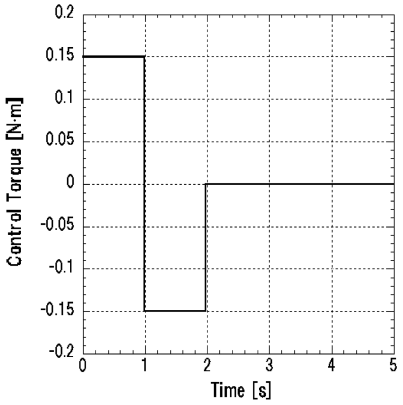

Fig. 10 Time history of control input torque for bang-bang control.

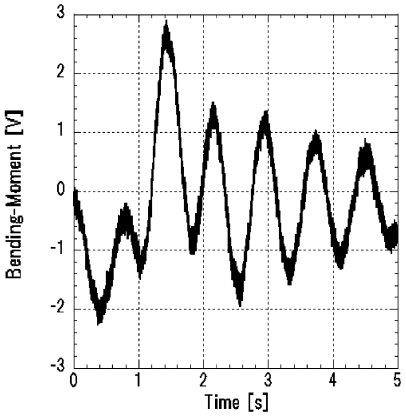

Fig. 11 Bending moment resulting from bang-bang control.

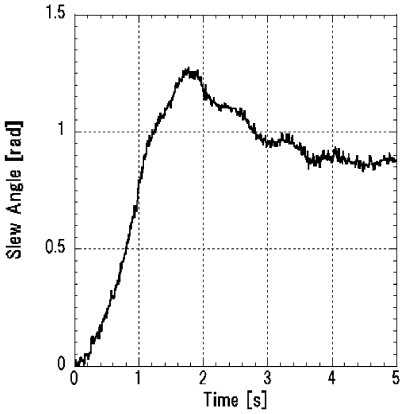

Fig. 12 Slew angle of the main body resulting from bang-bang control.

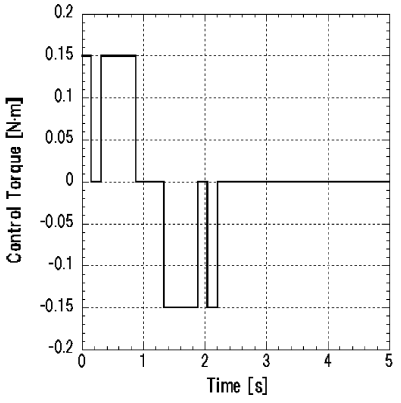

Fig. 13 Time history of control input torque for deflection-limiting control.

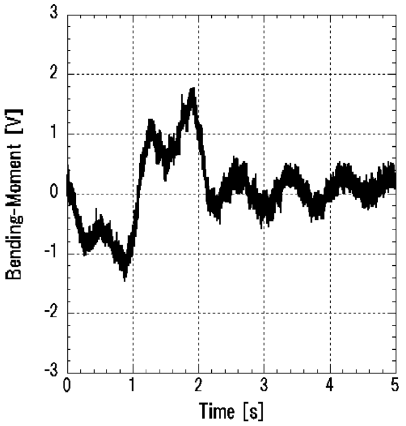

Fig. 14 Bending moment resulting from deflection-limiting control.

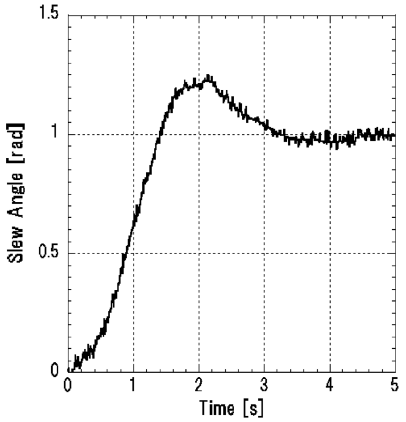

Fig. 15 Slew angle of the main body resulting from deflection-limiting control.

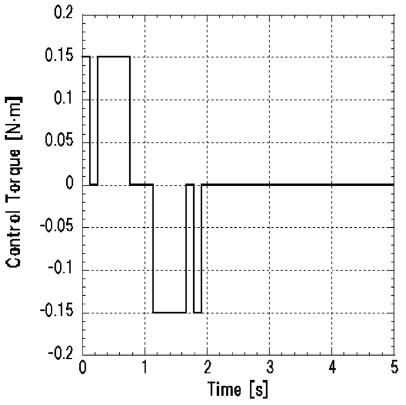

Fig. 16 Time history of control input torque for adaptive deflection-limiting control.

control is shown in Fig. 13, and the time response of the bending moment and slew angle for the DL control are shown in Figs. 14 and 15, respectively. Note that DL control does limit the transient deflection to approximately 60% and also greatly reduces residual vibration. Figures 16–18 show the time history of the control input, the bending moment, and the slew angle for the case of the ADL control. The slew angle decreases after the control process has finished for all the cases. This may be because the air drag affects the flexible appendage and the dynamic or static friction affects the shaft of the dc motor. Also some overshoot subject to the desired final angle occurred under bang-bang and DL control. This may be because the modeled inertia of the main body is different from the real value. On the other hand, the maximum slew angle for the ADL control does not exceed the desired final angle. This is because the

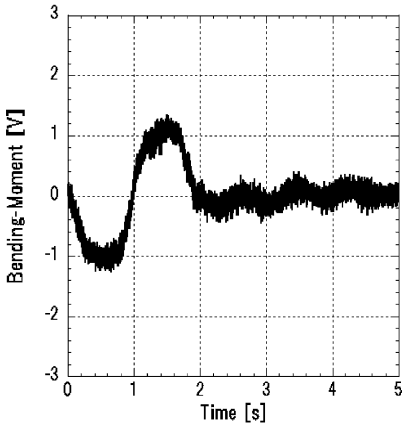

Fig. 17 Bending moment resulting from adaptive deflection-limiting control.

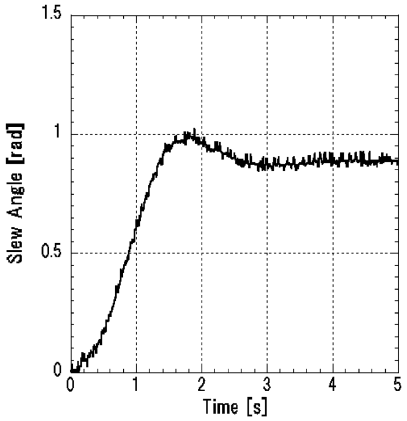

Fig. 18 Slew angle of the main body resulting from adaptive deflection-limiting control.

slew angle and angular velocity are monitored and the command switch times are tuned to achieve the desired slew angle.

The experimental results for the bang-bang control, DL control, and ADL control are summarized in Table 2. The residual vibration for the case of the ADL control is greatly reduced, compared to the case of bang-bang control. Furthermore, the maximum value of the bending moment is successfully reduced, compared to that of the DL control and bang-bang control. The results clearly demonstrate that the ADL control is effective at suppressing both the bending moment during maneuver and the residual vibration.

Table 2 Comparison of experimental results

	Maximum bending moment	Residual vibration
Bang-Bang	2.9 V (100%)	1.5 V (100%)
DL	1.8 V (62.1%)	0.6 V (40.0%)
ADL	1.4 V (48.3%)	0.4 V (26.7%)

V. Conclusions

An adaptive deflection-limiting control has been developed and applied to a rest-to-rest slew maneuver of a flexible structure. The flexible structure in this study is modeled as a rigid main body equipped with a flexible beam. The bending moment at the root of the beam is sensed by strain gauges and used to estimate the first modal frequency of the beam using the predicted ratio between the first and second mode frequencies. Experimental results show that even if the first frequency is not known in advance, the adaptive deflection-limiting control can effectively suppress the transient bending moment during the maneuver and the residual vibrations at the end of slewing. The control achieves this effect by tuning the time location and amplitude of the input shaper in accordance with the estimated first modal frequency and the relationship between the deflection limit and applied maximum control torque. Experimental results confirmed the effectiveness of the proposed method.

References

[1] Smith, O. J. M., *Feedback Control Systems*, McGraw–Hill, New York, 1958.

[2] Singer, N. C., and Seering, W. P., "Preshaping Command Inputs to Reduce System Vibration," *Journal of Dynamic Systems, Measurement, and Control*, Vol. 112, No. 1, 1990, pp. 76–82.

[3] Singhose, W. E., Seering, W. P., and Singer, N.C., "Input Shaping for Vibration Reduction with Specified Insensitivity to Modeling Errors," *Japan/USA Symposium on Flexible Automation*, ASME, New York, 1996, pp. 307–313.

[4] Singhose, W. E., Derezinski, S., and Singer, N. C., "Extra-Insensitive Input Shaping for Controlling Flexible Spacecraft," *Journal of Guidance, Control, and Dynamics*, Vol. 19, No. 2, 1996, pp. 385–391.

[5] Tzes, A., and Yurkovich, S., "An Adaptive Input Shaping Control Scheme for Vibration Suppression in Slewing Flexible Structures," *IEEE Transactions on Control Systems Technology*, Vol. 1, No. 2, 1993, pp. 114–121.

[6] Khorrami, F., Jain, S., and Tzes, A., "Adaptive Nonlinear Control and Input Preshaping for Flexible-Link Manipulators," *American Control Conference*, American Automatic Control Council, Evanston, IL, 1993, pp. 2705–2709.

[7] Bodson, M., "An Adaptive Algorithm for the Tuning of Two Input Shaping Methods," *Automatica*, Vol. 34, No. 6, 1998, pp. 771–776.

[8] Magee, D., and Book, W., "The Application of Input Shaping to a System with Varying Parameters," *Japan/USA Symposium on Flexible Automation*, ASME, New York, 1992, pp. 519–525.

[9] Fujii, A. H., Kojima, H., and Nakajima, N., "Slew Maneuver of a Flexible Space Structure with Constraint on Bending-Moment," *Journal of Guidance, Control, and Dynamics*, Vol. 26, No. 2, 2003, pp. 259–266.

[10] Kojima, H., and Nakajima, N., "Multi-Objective Trajectory Optimization by a Hierarchical Gradient Algorithm with Fuzzy Decision Logic," *Transactions of the Japan Society for Aeronautical and Space Sciences*, Vol. 47, No. 155, 2004, pp. 66–74.

[11] Singhose, W., Banerjee, A., and Seering, W., "Slewing Flexible Spacecraft with Deflection-Limiting Input Shaping," *Journal of Guidance, Control, and Dynamics*, Vol. 20, No. 2, 1997, pp. 291–298.

[12] Robertson, M., and Singhose, W., "Closed-Form Deflection-Limiting Commands," *Proceedings of the American Control Conference*, Vol. 3, IEEE, Piscataway, NJ, 2005, pp. 2104–2109.

[13] Ljung, L., *System Identification Theory for the User*, Prentice–Hall, Englewood Cliffs, NJ, 1987, p. 146.